Changes in a Phospholipid Bilayer Induced by the Hydrolysis of a Phospholipase A_2 Enzyme: A Molecular Dynamics Simulation Study

Marja T. Hyvönen,*† Katariina Öörni,† Petri T. Kovanen,† and Mika Ala-Korpela†
*NMR Research Group, Department of Physical Sciences, University of Oulu, FIN-90014 Oulu, Finland, and †Wihuri Research Institute, FIN-00140 Helsinki, Finland

ABSTRACT Phospholipase A_2 (PLA_2) enzymes are important in numerous physiological processes. Their function at lipid-water interfaces is also used as a biophysical model for protein-membrane interactions. These enzymes catalyze the hydrolysis of the *sn*-2 bonds of various phospholipids and the hydrolysis products are known to increase the activity of the enzymes. Here, we have applied molecular dynamics (MD) simulations to study the membrane properties in three compositionally different systems that relate to PLA_2 enzyme action. One-nanosecond simulations were performed for a 1-palmitoyl-2-linoleoyl-*sn*-glycero-3-phosphatidylcholine (PLPC) bilayer and for two of its PLA_2-hydrolyzed versions, i.e., bilayers consisting of lysophospholipids and of either free charged linoleate or free uncharged linoleic acid molecules. The results revealed loosening of the structure in the hydrolyzed bilayer due to increased mobility of the molecules in the direction normal to the bilayer. This loss of integrity due to the hydrolysis products is in accord with observations that not only the presence of hydrolysis products, but also a variety of other perturbations of the membrane may activate PLA_2. Additionally, changes were observed in other structural parameters and in the electrostatic potential across the membrane-water interface. These changes are discussed in relation to the simulation methodology and the experimental observations of PLA_2-hydrolyzed membranes.

INTRODUCTION

Phospholipases A_2 (PLA_2) are a heterogeneous group of enzymes involved in a variety of physiological processes, such as host defense and signal transduction. Mammalian PLA_2 enzymes can be classified into three large groups, namely secretory, cytosolic, and Ca^{2+}-independent enzymes (Murakami et al., 1997). The function of PLA_2 is to catalyze the hydrolysis of the *sn*-2 bond in various phospholipids, i.e., to generate a fatty acid and a lysophospholipid molecule.

Because of the central role of PLA_2 enzymes in mammalian physiology, a number of studies have focused on the mechanisms of their action. Particularly, the secretory type II PLA_2 has been studied extensively. The results have revealed that in addition to the properties of the interfacial binding surface of the enzyme (Gelb et al., 1999), the characteristics of the membrane itself are critical for the regulation of the enzyme activity (reviewed by Burack and Biltonen, 1994; Burack et al., 1997). The positively charged type II PLA_2 is known to interact preferentially with negatively charged membrane surfaces (Volwerk et al., 1986; Ghomashchi et al., 1991; Scott and Sigler, 1994; Han et al., 1997). In addition, various surface defects or perturbations caused, for example, by lipid peroxidation (McLean et al., 1993), by a change to the main phase transition temperature of the substrate (Jain and Jahagirdar, 1985; Bell et al., 1996; Hønger et al., 1996), by osmotic stress (Lehtonen and Kinnunen, 1995), by incorporation of diacylglycerol (Bell et al., 1996) or lysophospholipids (Jain and de Haas, 1983), or even by pressure from the tip of the atomic force microscope (Grandbois et al., 1998) are known to activate PLA_2.

Control of the action of water-soluble phospholipases on membranes is an important regulatory mechanism for preventing the degradation of intact biomembranes (Waite, 1996). Thus, zwitterionic phosphatidylcholine (PC) molecules, the main lipid constituents of biomembranes, are poor substrates to PLA_2 in an intact membrane. In pure PC membranes, this often results in a lag phase of low initial PLA_2 activity. However, after this initial lag phase, a sudden increase can occur in the enzyme activity (Burack and Biltonen, 1994). Much evidence suggests that this abrupt increase in PLA_2 activity is due to the accumulation of hydrolysis products, i.e., fatty acid and lysophosphatidylcholine (lyso-PC) molecules (Apitz-Castro et al., 1982; Bell and Biltonen, 1992; Burack et al., 1993; Sheffield et al., 1995; Bent and Bell, 1995; Bell et al., 1996; Henshaw et al., 1998). Yet, despite a wide variety of experiments designed to study the mechanisms underlying sudden PLA_2 activation, the detailed molecular interactions still remain unclear. Therefore, it would be important to aim at better understanding the relationship between the local structural characteristics of the membrane and the activity of the enzyme. Such detailed understanding of this relation would also be useful in a more general sense, since the PLA_2-membrane complex is a commonly used biophysical model system for protein-membrane interactions (Burack and Biltonen, 1994; Hønger et al., 1996).

Molecular dynamics (MD) simulations have been increasingly used to gain information about various membrane-related phenomena at the molecular level (Tieleman

Received for publication 7 April 2000 and in final form 24 October 2000.
Address reprint requests to Dr. Mika Ala-Korpela, Wihuri Research Institute, Kalliolinnantie 4, 00140 Helsinki, Finland. Tel.: + 358-9-4582810; Fax: + 358-9-637476; E-mail: neurotuotanto@kolumbus.fi.

0006-3495/01/02/565/14 $2.00

et al., 1997; Tobias et al., 1997). For example, MD simulation studies have addressed the molecular mechanisms of diffusion (Bassolino-Klimas et al., 1995) and channel-independent ion transport across membrane bilayers (Marrink et al., 1996; Wilson and Pohorille, 1996). The membrane-associated peptides and proteins (Belohorcová et al., 1997; Tieleman and Berendsen, 1998) and the effects of polyunsaturation (Hyvönen et al., 1997) have also been studied. In addition, MD simulations have been utilized in a preliminary study of monolayer-PLA_2 interaction (Berendsen et al., 1992) and to investigate a PLA_2-substrate complex (Jones et al., 1993) and interactions between the PLA_2 molecule and an intact dilaurylphosphatidylethanolamine (DLPE) membrane (Zhou and Schulten, 1996). The last mentioned study showed that, as compared with a loosely bound PLA_2-membrane complex, desolvation of lipids in a tightly bound complex enhances the interaction between the enzyme and the phospholipids. The results of Zhou and Schulten (1996) also suggested that the PLA_2-membrane interactions would be sensitive to various changes produced in the membrane, which appeared to be more important in controlling PLA_2 activity than the conformational changes in the enzyme itself. However, there seems to be no direct information on the effects of PLA_2 hydrolysis products on the membrane structure.

In this study we aimed at revealing changes in the membrane characteristics due to the presence of the PLA_2 hydrolysis products. As MD simulations are suitable for studies in which structural effects due to the compositional changes are investigated, we focused on the structural differences between a phospholipid bilayer and its counterparts consisting of the PLA_2 hydrolysis products. To the best of our knowledge, this is the first time that MD simulations have been applied in this way for assessing the structural changes in a membrane induced by a lipid-hydrolyzing enzyme. We performed three 1-ns MD simulations: one for a 1-palmitoyl-2-linoleoyl-*sn*-glycero-3-phosphatidylcholine (PLPC) bilayer and two for its PLA_2 hydrolyzed versions, in which the *sn*-2 chains were liberated either as charged linoleate or uncharged linoleic acid molecules. The constituents from all of these simulations are present in a real partly hydrolyzed membrane, as in the physiological pH both charged and uncharged hydrolysis products appear (Hamilton, 1995) together with the lysophospholipids and remaining unhydrolyzed lipid molecules. The main observation in the hydrolyzed bilayers was a loosened structure of the membrane in the direction normal to the bilayer. In addition, the structural parameters of the headgroups, water molecules, glycerol backbone, and chains were determined together with the electrostatic potential across the membrane-water interface. The results will be discussed in relation to the applied simulation methodology and the experimental observations on PLA_2-membrane interrelations.

METHODS

Modeling and computational details

The molecules used in the three simulated bilayer systems are shown in Fig. 1. The PLPC molecule, used in the first bilayer system, consists of a glycerol backbone (Cg1–Cg3) to which the saturated palmitate chain (16:0), the diunsaturated linoleate chain ($18:2^{\Delta 9,12}$), and the PC headgroup are attached at the *sn*-1, *sn*-2, and *sn*-3 positions, respectively. In the second system, as the PLA_2 enzyme is known to catalyze the hydrolysis of the *sn*-2 fatty acid bond, the bilayer consisted of lyso-PC molecules (a PC headgroup, glycerol backbone, and palmitic acid chain), and free negatively charged linoleate chains. In the third system the free *sn*-2 chains were protonated and appeared thus as uncharged linoleic acid molecules. At the physiological pH 7.4, both charged linoleate and uncharged linoleic acid molecules are expected to appear in nearly equivalent amounts (Hamilton, 1995). Thus, in a real phospholipid membrane the effects of both charged linoleates and uncharged linoleic acids are present. For simplicity, the linoleate and the linoleic acid molecules of the modified systems are here referred to as the *sn*-2 chains, although they are actually independent molecules.

The bilayer model of the PLPC molecules was based on the final structure of our earlier PLPC simulation (Hyvönen et al., 1997), where the bilayer was modeled implicitly by applying a "rotation-reflection" to the monolayer system. Here, to model the bilayer explicitly, the monolayer system was copied and placed similarly to the image of the monolayer in the implicit bilayer model. Additionally, a 1.25 Å slice from both water layers was removed, which resulted in the dimensions of 50.4 Å $\times$ 71.0 Å $\times$ 50.4 Å in *x*, *y*, and *z* axes, respectively. Thus, the system consisted of 72 PLPC molecules in the bilayer and a total of 2572 water molecules. Conventional periodic boundary conditions were used to model an infinite bilayer. The system was stabilized by energy minimization. Dynamic heating was then applied for a 10-ps period, resulting in a temperature of 310 K, followed by a 150-ps equilibration period and a simulation of 1 ns. This simulation was, however, affected by a typing mistake in the parameter file, which restricted the rotation of the single bonds between the double bonds. Thus, this simulation was not used for the analysis; instead, its final structure was taken as the starting point for the actual simulation with corrected parameters. Again, an energy minimization, a 10-ps heating period, and a 100-ps equilibration period were used. As the bilayer model was originally well-equilibrated (Hyvönen et al., 1997) and was further stabilized in the rejected simulation, this latter equilibration period was very stable. Finally, the simulation was run for 1 ns to collect the data reported here. The temperature and the energies were monitored during the simulation to ensure their stability and an adequate time for equilibration. The average temperature in the final 1-ns simulation was 310.25 K.

For the second system, the construction of the modified bilayer with lysophospholipids and charged free linoleic acid molecules was based on a well-equilibrated structure from the PLPC bilayer simulation. First, the bond between the glycerol backbone carbon Cg2 and the corresponding oxygen was cut and an OH group was added to Cg2, which resulted in separation of the linoleate and lysophospholipid molecules. To remove extensive overlaps of atoms in the modified region near the Cg2 carbon, the energy was minimized at this stage. In order to end up with an uncharged system, 72 water molecules evenly distributed at the headgroup regions were chosen and replaced by Na^+ ions. The energy was again minimized for the whole system. As in the case of the PLPC system, the first simulation was rejected from the analysis because of an erroneous parameter mentioned above, and the final structure was accepted for the new energy minimization with correct parameters. This minor error in the parameter file allowed us to stabilize the system extremely well. Also, at this point the distributions of Na^+ ions were calculated in order to compare them with the final distributions, and thus to ensure the convergence of the ion distribution. Finally, this was followed by a 10-ps period of dynamic heating to a temperature of 310 K and an equilibration period of 109 ps.

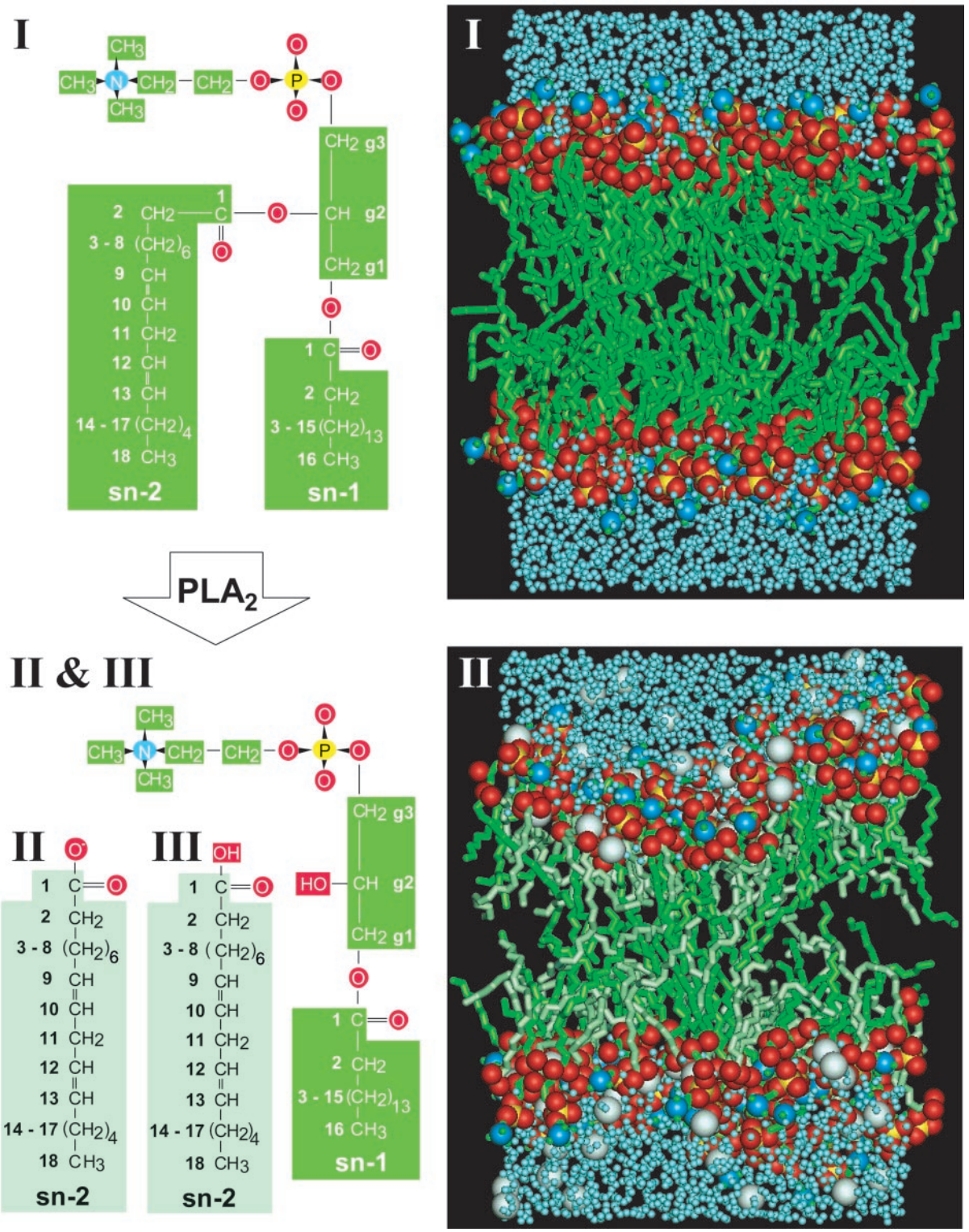

FIGURE 1 Snapshots from the first (I) and second (II) simulations of the PLPC system and of the system consisting of the lyso-PCs, charged linoleates, and Na^+ ions, respectively. Additionally, illustrations of the molecules in the first (I), second (II), and third (III) systems are shown: a single PLPC molecule (I) and, after the PLA_2 hydrolysis, a lyso-PC (II and III), charged linoleate (II), and uncharged linoleic acid (III) molecules. Water molecules are shown in cyan, Na^+ ions in grayish, and the color coding of the lipid molecules is as follows: green for carbon, red for oxygen, yellow for phosphorus, and blue for nitrogen. For clarity, the hydrogen atoms are not shown. The *y* axis is along the normal of the membrane.

The simulation reported here was run for 1 ns and the average temperature was 310.28 K.

The initial structure of the third bilayer system was based to the well-equilibrated structure from the PLPC bilayer simulation. The structural modifications were performed as in the second system to form lysophospholipids and free fatty acids, except that instead of COO^- the uncharged COOH group was formed, and no Na^+ ions were added. Thus, this bilayer model did not contain charged species. After the construction, the energy of the system was minimized, followed by the heating period of 10 ps, equilibration period of 195 ps, and finally the simulation was run for 1 ns in an average temperature of 313.78 K. In this third simulation, as it was performed after the first and the second simulations, the correct parameters for the double bond region were applied, and thus there was no need to repeat the simulation.

All simulations were performed in a microcanonical (NVE) ensemble using the parallel version, 25b2, of CHARMM software (Brooks et al., 1983). The use of a constant volume ensemble assumed that the release of the *sn*-2 fatty acid from the phospholipid does not significantly change the surface area per lipid molecule. Surface tension, as calculated frame by frame according to Venable et al. (2000) from the last 30 ps of each simulation, showed an essentially similar kind of behavior for all three systems. In the PLPC system, the same lipid force field parameters were used as have been reported earlier (Schlenkrich et al., 1996; Hyvönen et al., 1997), and these were also adapted for the linoleate, linoleic acid, and lysophospholipid molecules. Because the COO^- and COOH groups were not present in the lipid force field, the parameters for them were adapted from the CHARMM parameter set for amino acids. For water molecules, the TIP3P parameters (Jorgensen et al., 1983) were used. Every atom was taken into account independently in the MD simulations. The lengths of the bonds involving hydrogen atoms were fixed using the SHAKE algorithm with 10^{-9} tolerance, which allows the use of a 1-fs time step (van Gunsteren and Berendsen, 1977). The long-range interactions were truncated using an atom-based cutoff radius of 13 Å with a shifting function for the electrostatic and a switching function for the van der Waals interactions (Brooks et al., 1983). Especially in the case of charged species the truncation of electrostatic interactions involves risks. However, we would like to point out that in the simulations of charged membrane species, the truncation has been applied without noted artifacts (Lopez Cascales et al., 1996a, b; Wymore and Wong, 1999). To test the effect of cutoff distance, we performed an additional 0.5 ns simulation for the second system using a cutoff distance of 18 Å for electrostatic interactions. The second system contains charged species and should thus be most sensitive in this respect. However, the results calculated for the atomic distribution in the direction normal to the bilayer, for the orientational behavior of the headgroups and water molecules, and for the electrostatic potential showed essentially similar behavior in the simulations with cutoff distances of 13 Å and 18 Å (data not shown). The third simulation was performed with the uncharged hydrolysis products. Thus, it serves as an additional opportunity to explore which results from the second simulation are related to the presence of charged species, and thus might be affected by the truncation of electrostatic interactions.

The nonbonded interactions were updated at every 10th step (0.01 ps). Energies, coordinates, and velocities were saved at every 50th step. The simulations were carried out using 64 processors of a Cray T3E computer at the Center for Scientific Computing, Espoo, Finland.

Data analysis

In the subsequent analysis, the averages were calculated over all saved time steps (20,000) of the 1-ns simulations and over all PLPC, linoleate, linoleic acid, lysophospholipid, or water molecules, unless otherwise stated.

Atomic single particle distribution functions in the direction normal to the bilayer were evaluated by calculating the total amount of each atom in 0.25 Å-thick slices. The distributions were averaged over time. The orientation angles of the headgroup and glycerol backbone vectors with respect to the bilayer normal and the angle distributions were determined from 1° slices. Here, the positive direction of the bilayer normal in both the upper and the lower layer was toward the water region.

The radial distributions of the oxygen and hydrogen atoms of the water molecules around the phosphorus and nitrogen atoms of the phosphatidylcholine headgroups were averaged for a 20-ps period from the end of the simulations, using the SCARECROW software (Laaksonen, 1992). In addition, similar calculations were performed for the water molecules around the carbon atoms of the COO^- and COOH groups of linoleate and linoleic acid, respectively, and for the Na^+ ions around the PC and COO^- headgroups.

The mean cosine of the angle between the water dipole moment vector and the bilayer normal in 0.25 Å slices along the bilayer normal was also calculated. A zero value is obtained for a random orientation and a negative value corresponds to the orientation of the dipole toward the bilayer center at positive values of y, while with negative values of y the positive value of the mean cosine corresponds to the orientation toward the center.

The orientational order is described by the order parameter S_j, which is defined as

$$S_j = \frac{1}{2}\langle 3\cos^2\beta_j - 1\rangle, \quad (1)$$

where β_j is the angle between the orientation vector and the reference direction. The brackets denote both the ensemble and time average. The ^{2}H-NMR-observable order parameter, S_j^{CD}, is obtained by defining the orientation vector along the CH_j bond, with the bilayer normal as the reference direction. Using this definition, we calculated the order parameters for all CH bonds. At each saturated carbon atom in the chains the S_j^{CD} value was taken as an average of the CH_j bonds. The standard error of the mean (SEM) of the 72 molecular averages is taken as an error estimate. For each of the molecules, the molecular average was evaluated from the whole time series of 1 ns. In this way, the effect of high correlations between consecutive time steps was eliminated, the error estimates then being more realistic. It is a convention in MD simulations to define the orientation vector along the normal of the HC_jH plane or from C_{j-1} to C_{j+1}, which leads to the molecular order parameter S_j^{mol}. When isotropic rotations around the HC_jH plane normal are assumed, the CH bonds and corresponding S_j^{CD} values become equivalent, and S_j^{CD} can be compared with the S_j^{mol} values according to the relation $-2S_j^{CD} = S_j^{mol}$ (Seelig and Niederberger, 1974). The S_j^{mol} may vary between $-½$ and 1, corresponding to the variation between perpendicular (90°) and parallel (0°) orientations with respect to the bilayer normal. Usually, a zero value of S_j indicates isotropic orientation distribution but, for example, a single orientation angle of 54.7° in the sample also results in a zero value.

The orientational angle distribution of the C1–C3 vectors of the chains was calculated with respect to the bilayer normal. Note that here the bilayer normal was considered to point toward the bilayer center, in contrast to the determination of the orientational distributions in the headgroup and glycerol backbone regions. This was done to keep the numerical values mainly below 90°.

The fractions of the *gauche*$^+$ (g^+), *gauche*$^-$ (g^-), and *trans* (t) states were determined for the dihedral angles of the glycerol backbone, the headgroup, and both chains. The angles were allocated to the appropriate state, using the ranges -120–0 and 0–120° for the g^+ and g^- states, respectively, and the rest for the t states. A similar allocation was used for evaluating the rate of isomerization among the g^+, g^-, and t states for each bond. The isomerization rate was averaged over all the molecules. For the two single bonds between the double bonds, the values of the dihedral angles were monitored during the simulation and the percentage distribution of conformations with different combinations of these angles was also determined.

Electrostatic potential profile along the bilayer normal y was calculated

based upon Poisson's equation

$$\psi(y) - \psi(0) = -\frac{1}{\varepsilon_0}\int_0^y \int_0^{y'} \rho(y'')dy''\,dy' \qquad (2)$$

where $\psi(y)$ is the electrostatic potential, $\rho(y)$ is the charge density at y, and ϵ_0 is the vacuum permittivity. The charge density was determined in 0.25 Å thick slices and averaged from the monolayers. The position $y = 0$ resides in the middle of the bilayer.

RESULTS AND DISCUSSION

The reaction products of PLA_2 action are known to play a particularly important role in the catalytic activity of PLA_2, and therefore the current MD simulations were set up to address these product-related changes. However, none of the present simulations alone can produce information that could be directly related to the function of a PLA_2 in a membrane. The three model systems should merely be considered to represent the features present in the partly hydrolyzed membranes. Therefore, this kind of combination of MD simulations is able to provide information at the molecular level and help in the interpretation of the hydrolysis-induced effects on membrane structure. To our knowledge, this is the first MD simulation study in which the action of the enzyme has been addressed without modeling the enzyme itself, and it thus also serves as a pilot study for an approach of this kind.

Our earlier study of the intact PLPC bilayer includes a detailed discussion of the properties of the PLPC membrane in the MD simulation in comparison to experiments and other simulations of phospholipid membranes (Hyvönen et al., 1997). The properties of the intact PLPC system are therefore not within the scope of the present analysis and discussion. Instead, detailed information on the structural differences between the intact PLPC system and its modified versions are provided by comparing them in light of the analysis of the general membrane structure and the different structural parts of the systems: the PC headgroup, glycerol backbone, hydrocarbon chains, water molecules, and Na^+ ions. In addition, the electrostatic potential profiles along the bilayer normal are compared.

General membrane structure

Snapshots from the end of the first and second simulations, i.e., PLPC bilayer and the bilayer of lyso-PCs and charged linoleate molecules, are shown in Fig. 1. These snapshots illustrate a marked difference between the overall structure of the systems: in the intact PLPC bilayer the structure is well defined, but in the modified bilayer of linoleate and lysophospholipid molecules the integrity of the membrane is seemingly weakened. In addition, in the PLPC bilayer, the choline groups mainly point toward the water region, but in the modified system their orientation has clearly changed, as some of them are found buried in the membrane. For the modified bilayer consisting of the lyso-PCs and uncharged linoleic acids, the snapshot is not shown because the overall structure of the system is quite close to the intact PLPC bilayer and the differences are not evident by visual inspection only.

In order to monitor the general structure of the bilayer systems in detail, the atomic single-particle distributions were calculated in the direction normal to the bilayer. The distributions are shown for several atoms in Fig. 2. The distributions are wider for the modified systems than for the PLPC bilayer. However, the effect is significantly enhanced in the second system of the lyso-PCs and charged linoleates. The distributions were also essentially similar for the second system in the test simulation (data not shown) with a larger cutoff distance for electrostatic interactions (see Methods). The wider distributions imply an increased mobility of the molecules in the direction normal to the bilayer.

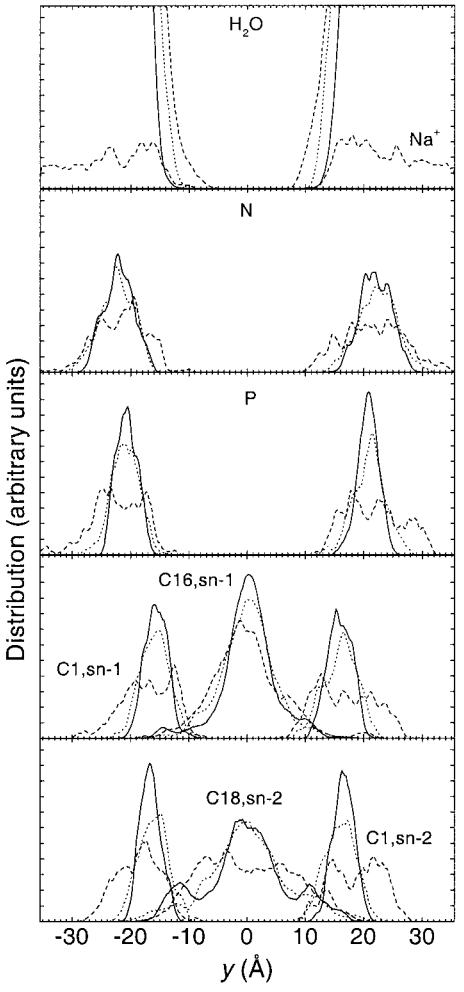

FIGURE 2 Distributions of water molecules, Na^+ ions, nitrogen, phosphorus, *sn*-1 chain carbons C1 and C16, and *sn*-2 chain carbons C1 and C18 along the bilayer normal of the first (—), second (- - -), and third (· · · ·) system.

The average distances of the phosphorus and nitrogen atoms from the bilayer center are 20.7 and 22.0 Å for the PLPC system (the first system), 22.0 and 21.8 Å for the second system, and 21.0 and 22.4 Å for the third system, respectively. Thus, a change in the orientation of the headgroup and also a change in the average membrane thickness is observed in the second system containing charged linoleate molecules, whereas in the case of third system only a slight change in the thickness is observed.

The average distances of the chain carbons from the bilayer center in the second system showed shifts of the lyso-PC (*sn*-1 chain) and charged linoleate (*sn*-2 chain) molecules toward the water region as compared with the intact PLPC bilayer (data not shown). However, in the third system only a slight shift toward the water region was observed for the lyso-PC and, contrary to the linoleate, the linoleic acid molecules slightly shifted (<1 Å) toward the center of the bilayer. In this shift, the last three carbons remained almost at the same height as their counterparts in the PLPCs, which might be due to enhanced tilt at the end parts of the chains. The descend of the unionized fatty acid toward the hydrophobic region has been observed using fluorescent probes (Abrams et al., 1992) and has been suggested to enhance the separation of the headgroups, which would allow the PLA_2 active site greater access to the *sn*-2 bond of the phospholipids (Henshaw et al., 1998).

The distribution of water in the three systems differs, as in the modified systems the water molecules have penetrated deeper into the bilayer interior than in the intact PLPC bilayer. The region that was free of water molecules in the bilayer center was ~20 Å in the first system of PLPC molecules and 10 Å and 16 Å in the second and third systems, respectively. Thus, the penetration of the water molecules toward the bilayer center is especially enhanced in the bilayer with charged linoleate molecules. The changes in the water penetration might also lead to changes in the diffusion of small molecules through the modified membrane systems. The change in the water penetration is an additional indication of the loosening of the structure in the modified membranes. In fact, there are studies of the membrane structure during the PLA_2 action (and accumulation of reaction products) with the fluorescent probe Prodan (Sheffield et al., 1995), which is sensitive to the polarity of its immediate environment in the headgroup region. The results indicated that disruption of the membrane structure was sufficient to allow increased ingress of water molecules near the Prodan probe.

In a partly hydrolyzed real phospholipid membrane, both charged and uncharged liberated *sn*-2 chains are present together with the lysophospholipids and the unhydrolyzed phospholipids. The results of the present simulations suggest that the presence of the hydrolysis products causes loosening of the bilayer structure. Loosening of the structure observed in our simulations with fully hydrolyzed membrane area suggests that most likely some loosening would also result in a partly hydrolyzed membrane system. This would enhance the mobility of PLPC substrate molecules in the membrane normal direction, which might increase diffusion of the substrate to the active site of the PLA_2 enzyme. Interestingly, the addition of the lyso-PC has been observed to enhance the availability of the substrate to the active site of the enzyme (Sheffield et al., 1995; Henshaw et al., 1998). In addition, the shift of the uncharged fatty acid molecules toward the bilayer center might also have a role in allowing the PLA_2 active site greater access to the *sn*-2 bond of the phospholipids (Henshaw et al., 1998). However, the loosening of the structure may facilitate penetration of PLA_2 amino acid side chains into the membrane and thus promote the tighter PLA_2–membrane complex (Zhou and Schulten, 1996). Interestingly, not only the accumulation of reaction products (Apitz-Castro et al., 1982; Burack et al., 1993, 1995, 1997; Sheffield et al., 1995; Bell et al., 1996; Henshaw et al., 1998), but also several manipulations of zwitterionic bilayers are known to enhance the catalytic rate of PLA_2. These manipulations include a change to the main phase transition temperature of the substrate (Jain and Jahagirdar, 1985; Bell et al., 1996; Hønger et al., 1996), osmotic stress (Lehtonen and Kinnunen, 1995), incorporation of diacylglycerol (Bell et al., 1996) or lyso-PC (Jain and de Haas, 1983), and perturbation with the atomic force microscope tip (Grandbois et al., 1998). The manipulations that activate PLA_2 appear to operate via different mechanisms and cause various perturbations in the bilayer. Hence, there is no necessity for a specific alteration in the PLA_2-prone areas of the membrane, but a certain degree of loosening of the structure of the intact membrane is sufficient to activate PLA_2.

The PC headgroup

The general electrostatic properties of the membrane are affected by the orientation of the headgroups. Differences in the average atomic distances of the phosphorus and nitrogen atoms from the bilayer center were already noted between the first and second systems (Fig. 2). To monitor the orientation in greater detail, the average angle distribution of the P–N vector was calculated with respect to the bilayer plane.

A comparison of the angle distributions between the intact PLPC and the modified systems is given in Fig. 3. In the PLPC system the PC headgroup, on average, orients slightly toward the water region, and the values for the angle of the P–N vector are between -60 and 90°. Interestingly, the third simulation of the uncharged linoleic acids and lyso-PCs produces a very similar angle distribution with the first simulation. The average orientation angles for the P–N vector in the first and third systems were 17 and 18°, respectively, in accordance with the value of 18° estimated from the NMR and Raman studies of dipalmitoylphosphatidylcholine (DPPC) (Akutsu and Nagamori, 1991). Fig. 3 illustrates, however, that all angles are possible in the sec-

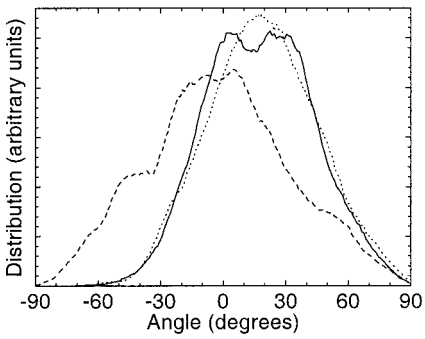

FIGURE 3 Averaged distribution of the orientation angles between the phosphorus-nitrogen vector and the bilayer normal of the first (—), second (- - -), and third (···) system. The positive direction of the bilayer normal is toward the water region.

ond system with charged linoleate and lyso-PC molecules, which reflects increased orientational freedom for the PC headgroups of the lyso-PC molecules. The average orientational angle of the P–N dipole was $-2°$ in this modified bilayer. The presence of charged linoleate molecules and Na^+ ions therefore caused a drastic change in the orientational behavior of the PC headgroups, resulting in a structure in which the choline groups were more often buried in the bilayer. This may be due to an enhanced interaction of the choline group with the COO^- of linoleate, which would cause the appearance of angles smaller than $-50°$.

One factor that has been shown to affect the PLA_2 activity is the presence of anionic lipids in the membrane, and the tight association between PLA_2 and interfaces containing anionic phospholipids is a general property of these enzymes (Volwerk et al., 1986; Ghomashchi et al., 1991; Han et al., 1997). In addition, Zhou and Schulten (1996) have proposed that negatively charged lipids, together with membrane defects considered above, might facilitate the penetration of a few enzyme residues into the membrane and thus cause the formation of a fully functional, i.e., tight, PLA_2–membrane complex. One established mechanism relating the accumulation of the PLA_2 reaction products, lyso-PC and fatty acid molecules, to the increased activity of the enzyme is the increased negative surface charge of the membrane due to the liberation of the *sn*-2 chains in the charged state. However, in the presence of the negatively charged linoleates the change in the orientational behavior of the PC-headgroups occurs so that the negatively charged phosphatidyl groups are now more accessible at the outermost surface of the membrane. They would thus be able to promote the negative surface charge originally caused by the linoleate molecules. These changes in the surface region of the membrane with charged species have to be considered in the light of the possible uncertainties produced by the truncated electrostatics applied in the simulation. However, the test simulation for the second system using a larger cutoff distance for electrostatic interactions (see Methods) resulted in a similar conclusion for the behavior of headgroups (data not shown).

Water and Na^+ ions

Radial distribution of water and Na^+ ions

The radial distributions of the oxygen and hydrogen atoms of the water molecules were calculated for all systems around the phosphorus and nitrogen atoms of the PC headgroups. In addition, for the modified bilayers, the radial distributions of the oxygen and hydrogen atoms of the water molecules were calculated around the COO^- group of linoleate and COOH group of linoleic acid, together with the radial distributions of the Na^+ ions around P, N, and COO^-. Since the radial distributions of the water molecules around P and N were very similar in all three systems, the distributions are shown in Fig. 4 from the second simulation only.

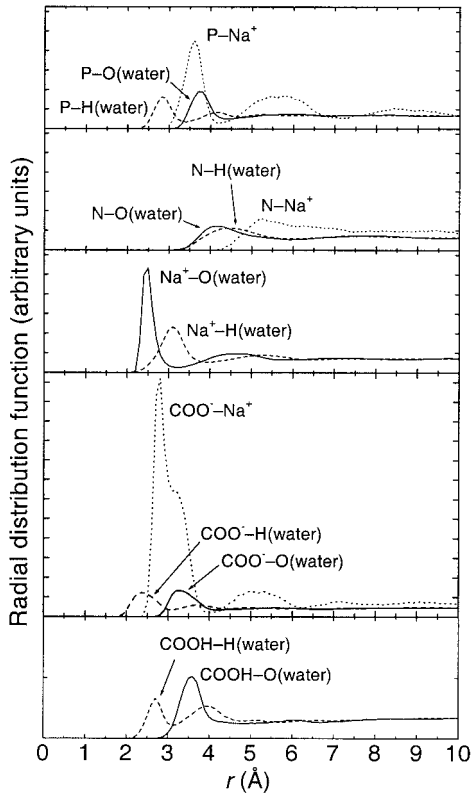

FIGURE 4 Radial distribution functions for the oxygen (—) and hydrogen (- - -) atoms of the water molecules and Na^+ ions (···) around the lysophospholipid phosphorus and nitrogen atoms and linoleate COO^- carbon atom, together with the radial distribution functions of the oxygen (—) and hydrogen (- - -) atoms of the water molecules around the Na^+ ions and linoleic acid COOH carbon atoms. The data for the last 20 ps of the simulation were averaged. As the system was anisotropic, the radial distribution functions do not approach one at the long separation limit and are therefore shown in arbitrary units. Note that in the lowest panel the tic separation corresponds to the one in the upper panels.

For all three systems, the water molecules were found to be strongly oriented around the phosphorus atom because of the hydrogen bonding between the oxygen atoms of the phosphatidyl group and the hydrogen atoms of the water molecules. Only a weak orientation is noticed around the nitrogen atom, despite the positive charge on the choline group. This is most likely due to the hydrophobic nature of the surrounding methyl groups, which results in hydrogen bonding among the water molecules. A very similar arrangement of water molecules around the PC headgroups has also been observed in other MD simulation studies of phospholipid systems (Alper et al., 1993; Damodaran and Merz, 1994; Essmann et al., 1995). In the modified bilayer of the second simulation, there is a clear structural arrangement of the Na^+ ions around the phosphorus atoms. The first narrow peak is most likely due to ionic interaction between the oxygen atoms of the phosphatidyl group and the Na^+ ions. The second and third peaks are wider and are probably affected by the interactions between the water molecules and the Na^+ ions. Around nitrogen, the Na^+ ions appear at a distance of $\sim$5 Å and, like the water molecules, do not show any clear structural arrangement.

The orientational behavior of the water molecules around the COO^- headgroup of linoleate and COOH group of linoleic acid is similar to the orientation around the phosphorus atom, when the peak interval between the hydrogen and oxygen distributions in each system is considered. However, the first peaks of the distribution functions appear at slightly varying intervals due to the differences between the group structures, and also, the intensity of the peaks around the COOH group are remarkably smaller than around COO^- and phosphorus due to the reduction in the amount of the water molecules nearby. Also, the addition of the hydrogen to the COOH group reduces the amount of water hydrogens pointing toward the oxygens. Naturally, the Na^+ ions also cause orientation of water molecules, i.e., the oxygen atoms of the water molecules point favorably toward the Na^+ ions. The Na^+ ions interact strongly with the COO^- headgroup, but the shape of the radial distribution function seems also to reflect an interaction between Na^+ and those water molecules that hydrogen-bond to the COO^- group. This distribution function, when compared with the corresponding sodium–carbon distribution function obtained from MD simulation of a sodium octanoate micelle in aqueous solution (Watanabe et al., 1988), is found to be very similar. Interestingly, in this micelle simulation the Ewald method was applied to treat electrostatic interactions.

Orientation of the water dipole with respect to the bilayer normal

The net orientation of the water dipole, together with the PC headgroup P–N dipole, also affects the general electrostatic properties of the membrane. Therefore, in Fig. 5, the profiles for the mean cosine of the angle between the water dipole moment vector and the bilayer normal in the intact PLPC system and the modified systems are compared. Both in the first and in the third simulation the water dipoles at the surface of the bilayer tend to orient toward the bilayer interior (Hyvönen et al., 1997). This is due to the strong orientation of the hydrogen atoms of the water molecules toward the phosphorus atoms, as indicated by the radial distribution functions in Fig. 4: as the number of hydrogen-bonded water molecules around the phosphatidyl group is larger on the side of the water region, the dominating orientation of the water dipoles is toward the bilayer center. Only a few water molecules penetrate into the hydrocarbon region, which results in poor statistics and a spiky profile. Similar orientational behavior of water molecules in the PC headgroup region has been reported, for example, in an MD simulation study of the dimyristoylphosphatidylcholine (DMPC) membrane (Chiu et al., 1995). Thus, the liberation of the *sn*-2 chain in the uncharged state does not seem to remarkably alter the orientational behavior of the water molecules at the membrane surface.

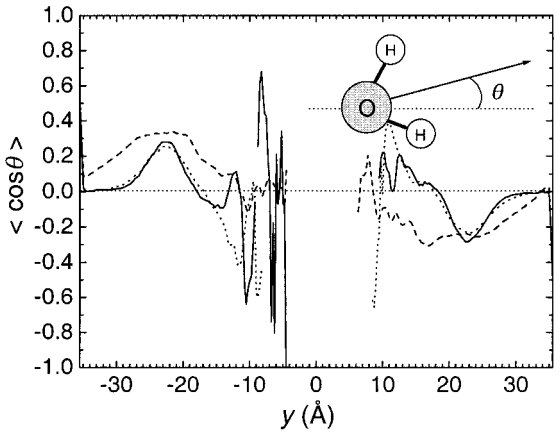

FIGURE 5 The mean cosine of the angle between the water dipole moment vector and the bilayer normal (y) for the first (—), second (- - -), and third ····) system.

In the second simulation for the lyso-PCs and charged linoleate molecules, the orientation of the water dipoles was seemingly different. There was no region of random orientation at $y > 30$ Å or $y < -30$ Å, since clearly oriented water extended over a much wider region than in the PLPC system. Over this wider range the orientation was also generally stronger than in the PLPC system. This can be assumed partly from the widened atomic distributions in the direction normal to the bilayer and partly from the fact that this modified system also includes water molecules oriented in a similar way to the phosphatidyl groups by the COO^- headgroups of linoleate molecules. The increased number of water dipoles orienting toward the interior of this linoleate-containing system means that, in practice, there are increased numbers of negatively charged oxygen atoms of the

water molecules pointing away from the membrane surface. It should be kept in mind, however, that the truncation of the electrostatics as done in the second simulation may enhance the ordering effect of the water molecules (Feller et al., 1996), especially in the system of charged species. However, at least increasing the cutoff distance to 18 Å in a test simulation of the second system (see Methods) did not reveal any major difference in the ordering of the water molecules (data not shown). It is tempting to speculate that this oriented water could affect the ability of PLA_2 to recognize the surface. However, the water orientation was not changed in the third system, which suggests that in real PLA_2 hydrolyzed membranes the possible effects to the water orientation would not be as prominent as observed here for the second system.

The glycerol backbone

The orientation angle distributions of the glycerol backbone bonds Cg1–Cg2 and Cg2–Cg3 with respect to the bilayer normal are shown in Fig. 6, together with the orientation of the Cg1–Cg3 vector. In the PLPC system, the Cg2–Cg3 bond is found in a more upward and more restricted orientation than the Cg1–Cg2 bond. In the modified systems, the Cg2–Cg3 bond has much more orientational freedom and the angle distribution of the Cg1–Cg2 bond has changed slightly. Thus, liberation of the *sn*-2 chains seems to allow perpendicular orientations of the Cg2–Cg3 bonds, but also shifts the Cg1–Cg2 bonds slightly toward orientations that are more parallel with the bilayer normal. Despite these differences in the orientation of the individual bonds of the glycerol backbone in the modified systems, there are only minor changes in the overall orientation of the glycerol backbone, as revealed by the orientation of the Cg1–Cg3 vectors in Fig. 6.

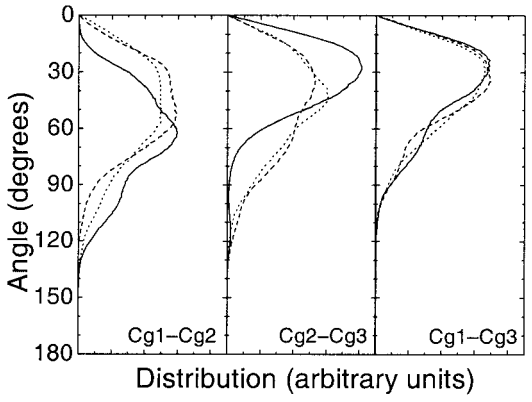

FIGURE 6 Distributions of the angles between the bilayer normal and the glycerol backbone vectors Cg1–Cg2 (*left*), Cg2–Cg3 (*center*), and Cg1–Cg3 (*right*) for the first (—), second (- - -), and third (· · · ·) system. The positive direction of the bilayer normal is toward the water region.

Chains

Orientational order parameters

The orientational order parameter profiles of the *sn*-1 and *sn*-2 chains of the PLPC and the modified bilayer systems are shown in Fig. 7. The profiles indicate a difference in orientational order near the beginning of the fatty acid chains between the intact PLPC system and the modified systems. After the beginnings of the chains, the differences gradually disappear, and toward the ends of the chains, the order parameters for the intact and modified bilayers become identical, except in the *sn*-2 chains in the third system, i.e., the linoleic acid molecules, where some change is observed at the double bond region and at the chain ends.

The differences between the orientational order parameters for the chains of intact PLPC and the modified systems are most likely related to a difference in the average conformation near the beginning of the chain. Although in the PLPC system the *sn*-1 chain begins, on average, more in the direction normal to the bilayer than the *sn*-2 chain, quite heavily tilted beginnings of the *sn*-1 chains are also observable, probably because the *sn*-1 and *sn*-2 chains are competing for the best packing option. However, in the PLPC bilayer, the *sn*-2 chains begin, on average, more in the plane of the bilayer than the *sn*-1 chains, and the beginnings of the *sn*-2 chains are therefore tilted. In the modified systems, in contrast, the chains can orient more freely in the direction of the bilayer normal and so result in increased $-S^{CD}$ values. This is clearly seen in Fig. 8, where the distributions of the angles between the C1–C3 vector and the bilayer normal are shown for *sn*-1 and *sn*-2 chains in all three systems. The

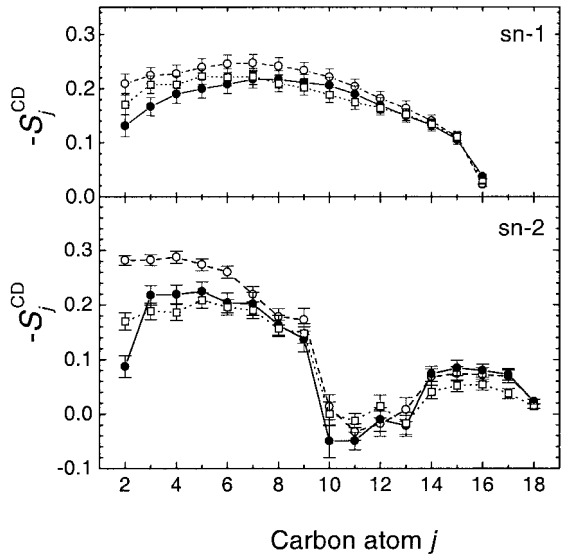

FIGURE 7 Averages of the $-S_j^{CD}$ orientational order parameters along the *sn*-1 and *sn*-2 chains of the first (●), second (○), and third (□) system. The SEMs of the molecular averages are shown as error bars for the values from the simulation.

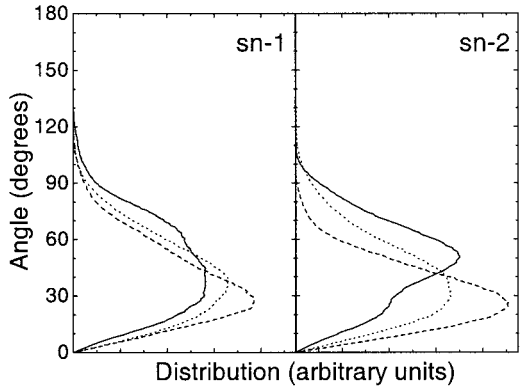

FIGURE 8 Distributions of the orientation angle between the C1–C3 vector and the bilayer normal for the *sn*-1 and *sn*-2 chains of the first (—), second (- - -), and third (· · · ·) system. Note that here the positive direction of the bilayer normal is toward the bilayer center.

strong increase in the order parameters in the beginning of the linoleate molecules of the second simulation is caused by a dramatic decrease in the amount of *gauche* states (data not shown), whereas other minor changes in the order parameters of the chain beginnings and of the double bond and the chain end regions of the linoleic acids are not reflected in the amount of *gauche* states. Also, the bond isomerization rates were very similar for the PLPC and the modified systems (data not shown). Thus, the minor changes are due, not to isomerization, but merely to slight orientational changes at the chain parts. For instance, the changes at the double bond and chain end regions of the linoleic acid chains occur near the zero value of the order parameter and could possibly be reflected by the above-mentioned slight shift of the linoleic acid molecules toward the bilayer center. Both the order parameter profiles and the angle distributions show that the effect on the chain beginnings is enhanced in the case of the second simulation of lyso-PCs and charged linoleates as compared to the third simulation of uncharged species.

In all, accumulation of PLA_2 hydrolysis products in the membrane seems to affect the orientational order of the fatty acid chains near the surface regions, but not remarkably in the interior of the membrane. This result is supported by the findings of Sheffield et al. (1995), who have utilized bis-pyrene fluorescence to sense the freedom of motion in the region of the hydrophobic core of the bilayer. They found no enhanced excimer-to-monomer ratio of bis-pyrene labels during or after the lag period of PLA_2 activity, i.e., the increase in enzyme activity required no remarkable changes in the order of the phospholipid acyl chains.

Structures of the double bond region

In an earlier paper we discussed the different internal structures of the double bond region in the PLPC membrane (Hyvönen et al., 1997). The internal structure of the double bond region is determined by the states of the single bonds between the double bonds, i.e., the dihedral angles over the bonds C10–C11 and C11–C12. These angles have values of $\sim\pm120°$. With the combinations of $+120/+120°$ and $-120/-120°$, the orientation of the double bonds with respect to the bilayer normal remains almost the same, whereas with the $+120/-120$ or $-120/+120$ combinations, the orientation between the double bonds changes by some 90°. In the first, second, and third simulations, 71%, 70%, and 66% of all the structures had the straight double bond region conformation, and the rest had the tilted conformation. This is in accordance with the similarity of the orientational order behavior at the double bond region in these systems. However, the 4–5% decrease in the amount of the straight conformations in the third simulation could be related to the noticed minor changes in the orientational order parameters at the double bond and chain end region and to the observations that the linoleic acid chains shift slightly toward the bilayer center.

Electrostatic potential across the membrane-water interface

The electrostatic potential profiles along the bilayer normal were calculated for all systems together with the separate contributions from the lipids and water, and are shown in Fig. 9. In the second simulation the contribution of the Na^+ ions is included into the lipid profile. A negative potential is observed in the water layer with respect to the bilayer center in all three simulations. The potential differences between the bulk water layer and the bilayer center are -2.6, -0.5, and -3.4 V for the first, second, and third systems, respectively.

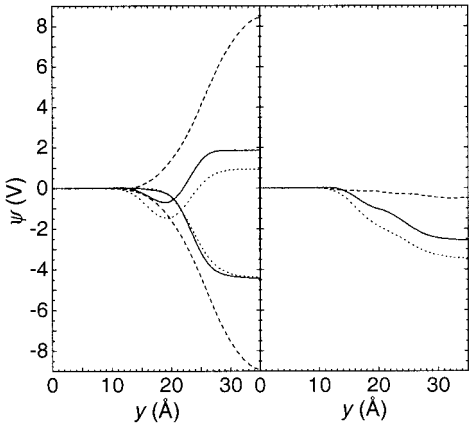

FIGURE 9 Electrostatic potential along the bilayer normal. The contributions (*left*) from the lipids (*three upper curves*) and water (*three lower curves*) together with the total potential profile (*right*) for the first (—), second (- - -), and third (· · · ·) simulations. The profiles are averaged over the monolayers and $y = 0$ corresponds the interior of the bilayer.

The potential of the intact PLPC bilayer can be compared with the other MD simulation studies for the phospholipids, which report the differences from −2.3 V to +0.5 V with varying methodology (Marrink et al., 1993; Chiu et al., 1995; Essmann et al., 1995; Berger et al., 1997; Tieleman and Berendsen, 1996; Feller et al., 1996; Shinoda et al., 1998; Essmann and Berkowitz, 1999), whereas experimental values range from −0.6 to −0.2 V (Gawrisch et al., 1992; Flewelling and Hubbel, 1986; Simon and McIntosh, 1989). Thus, the sign of the potential is generally reproduced, but the value is often overestimated in the simulations. Especially, the use of the spherical truncation has been concluded to cause extra ordering of the water (Feller et al., 1996), which enhances the negativity of the potential, and may account for the very negative potential observed here for the PLPC system. Other methodological aspects, such as the choice of the fractional charges, macroscopic boundary conditions, and water model, are also known to affect the electrostatic potential (Berger et al., 1997; Tieleman and Berendsen, 1996). That explains the wide variety in the potentials from the simulation studies. However, qualitatively the general behavior observed in other simulations is also reproduced here because the positive potential of several volts is produced by the lipids and overcompensated by the negative potential due to the ordering of the water dipoles. The negative dip around 19 Å in the lipid contribution is due to the orientation of the ester oxygens, which has also been observed by others (Berger et al., 1997; Essmann et al., 1995; Essmann and Berkowitz, 1999). The succeeding positive slope arises due to the orientation of the headgroup dipoles.

The potential profiles of the second bilayer system with the charged linoleate molecules and the Na^+ ions differ remarkably from the intact PLPC bilayer. The contribution from the lipids and the Na^+ ions reflects the compensation of the negative charges of the linoleate by the positive ions and by the changed orientational behavior of the headgroup dipole. Accordingly, the ordering of the water molecules is also strongly enhanced. However, due to the compensating effect of the water the total potential is small as compared to the simulation of the PLPC bilayer. Due to the loosened integrity the slope of the potential profile ranges near the box edges. The potential profiles for the second system were also determined from the test simulation with the increased cutoff distance for electrostatic interactions (see Methods). The profiles were also essentially similar with the larger cutoff distance (data not shown).

In the lipid contribution of the electrostatic potential from the third system, the negative dip around 19 Å is enhanced as compared to the PLPC bilayer. This is most likely related to the appearance of extra dipoles due to the liberation of the *sn*-2 chains. However, the contribution of the water ordering is nearly similar to the first system, causing a total potential that is even more negative than in the case of the PLPC bilayer. Interestingly, the measurements of the dipole potentials have revealed enhanced positive potential in the interior of the phospholipid-ketocholestanol membrane as compared to the phospholipid-cholesterol system, which was interpreted to be due to the orientation of an extra ketone dipole (Voglino et al., 1998). Thus, the situation qualitatively resembles the appearance of the extra dipoles in the third system, and their contribution to the total potential.

CONCLUSIONS

In this study we have addressed the structural effects induced in a phospholipid bilayer by an enzyme that hydrolyzes phospholipids at a membrane surface, namely PLA_2, but without including the enzyme molecule itself in the calculations. An approach of this kind is possible when applying MD simulations: if the result of the enzyme action on an individual substrate molecule is known, a system consisting partly or totally of the product molecules can be simulated and compared with a simulation of the intact system of substrate molecules. Here, we wanted to study the structural effects induced by PLA_2 hydrolysis on the membrane and therefore simulated and compared an intact bilayer and PLA_2-treated bilayers consisting totally of the hydrolysis products. To the best of our knowledge, this is the first time that MD simulations have been applied in this way for assessing the structural changes induced in a membrane by a lipid-hydrolyzing enzyme. This is not to be considered as a full computational approach to the questions related to the product-induced activation of the PLA_2 enzyme, but to serve as a new possibility to address the role of the membrane constituents in the membrane-enzyme interactions, in combination with other computational and experimental approaches.

Much evidence has accumulated to show that the PLA_2 hydrolysis products, i.e., fatty acid and lyso-PC molecules, cause an abrupt increase in the activity of the enzyme. This increase is generally attributed to the changes in the membrane characteristics. To study the structural effects of the hydrolysis products on the membrane at the molecular level, we performed three MD simulations: for an intact PLPC bilayer and for two of its modified counterparts consisting of the PLA_2 hydrolysis products, i.e., lyso-PCs and liberated *sn*-2 chains either as charged linoleate or uncharged linoleic acid molecules.

The simulation results revealed differences in the general bilayer structure: the PLA_2-hydrolyzed bilayers had a loosened structure in the direction normal to the bilayer as compared with the intact PLPC system. This was accompanied by increased penetration of the water molecules toward the bilayer center and by increased surface roughness. These effects were especially enhanced in the system with the charged species, but were also clearly noticeable in the bilayer of the uncharged hydrolysis products. The decreased integrity of the bilayers consisting of the hydrolysis prod-

ucts implies structural perturbations in the hydrolyzed bilayer area. Loss of integrity would also most likely appear in a partly hydrolyzed membrane. This is in accordance with the observations that, in addition to the presence of the hydrolysis products, varying perturbations may also activate PLA_2 by allowing more mobility of the substrate molecules in the membrane-normal direction and, accordingly, better access to the active site of the enzyme (Apitz-Castro et al., 1982; Jain and de Haas, 1983; Jain and Jahagirdar, 1985; Burack et al., 1993, 1995, 1997; Sheffield et al., 1995; Lehtonen and Kinnunen, 1995; Bell et al., 1996; Hønger et al., 1996; Henshaw et al., 1998; Grandbois et al., 1998). In addition, the surface defects have been suggested to help interdigitation of the enzyme residues to the membrane and facilitate better contact between the membrane and the enzyme (Zhou and Schulten, 1996). Here, in the bilayer system with the lyso-PCs and the uncharged linoleic acid molecules, the loosened integrity was seen to be accompanied by a slight shift of the linoleic acid molecules toward the bilayer center. This has also been observed experimentally and has been suggested to allow slight separation of the headgroups, which would further enhance the availability of the substrate to the active site of PLA_2 (Henshaw et al., 1998).

In addition, increases in the orientational order parameters of the chain beginnings were observed in the simulations, because liberation of the *sn*-2 chains allows the chain beginnings to orient more freely along the bilayer normal. There were also remarkable changes in the headgroup and in the water orientational behavior of the bilayer system with the lyso-PCs, charged linoleate molecules, and Na^+ ions. In all simulated systems the electrostatic potential was negative in the water region as compared with the membrane interior. Other simulation studies have suggested that this is due to the positive potential from the lipid molecules, which then would be overcompensated by the ordering of the water molecules (Tieleman and Berendsen, 1997; Tobias et al., 1997). This behavior was also qualitatively reproduced here. As truncation has been reported to enhance the ordering of the water molecules, the potential values obtained from the simulations cannot be considered to be quantitative. However, between the compositionally different bilayer systems studied here, the values of the total potential varied significantly, implying variability in the membrane potential due to the presence of hydrolysis products.

From the methodological point of view, we would like to emphasize that interpretation of the results for the second system should be done keeping in mind that, because of the presence of charged molecular species, the results may be affected by truncation of the electrostatics. Here the effect of enlarging the cutoff distance for electrostatic interactions from 13 to 18 Å was tested for the second system with charged species. The behavior was essentially the same with both cutoffs, suggesting that the treatment of electrostatic interactions was justified for the purposes of this study. Also, in a recent study of micelle-peptide interactions (Wymore and Wong, 1999), truncation of the electrostatics was applied to a system with charged species and no artifacts were noted. The radial distribution functions for the charged species in our second simulation are also similar to those reported earlier for the corresponding charged species in MD simulations using the Ewald method (Watanabe et al., 1988). Moreover, the third simulation without charged species, i.e., with lyso-PC and linoleic acid molecules, can be utilized to distinguish which results are related to the presence of the charged species and might thus be affected by the truncation. The current simulations were performed in a constant-volume ensemble, i.e., it was approximated that release of the *sn*-2 fatty acid from the phospholipid does not significantly change the surface area per lipid molecule. Surface tension, as calculated frame by frame from the end parts of the simulation, showed essentially similar behavior for all three systems, and thus, at least in this particular case, the approximation of a constant volume is well justified for the purposes of the study. Although presently the constant-pressure ensemble is often chosen, the methodological aspects are currently not clear. First, the question remains whether zero or non-zero surface tension should be used in constant pressure simulations (Feller and Pastor, 1996, 1999; Jähnig, 1996; Roux, 1996; Tieleman and Berendsen, 1996; Berger et al., 1997). Second, the different methods for constant pressure simulations may lead to surprisingly different areas per lipid, as has been indicated by the recent comparison of two commonly applied methods that resulted in an ~10% difference in the areas per lipid (Zubrzycki et al., 2000).

In general, the information obtainable on the detailed molecular changes in the membrane with the present MD approach could be of importance for studies on other lipid-hydrolyzing enzymes, since membrane structure is likely to be crucial in controlling the binding and activity of the enzyme, not only in the case of PLA_2 but also for other similar enzymes (e.g., phospholipase C, Basáñez et al., 1996). Thus, it will be of future interest to apply MD simulations for assessing the structural effects of the compositional changes in lipid membranes due to the action of various lipases.

We thank the Center for Scientific Computing (Espoo, Finland) for the computer resources. The Wihuri Research Institute is maintained by the Jenny and Antti Wihuri Foundation.

This work was supported by grants from the Academy of Finland (M. Ala-Korpela), the A. I. Virtanen Institute for Molecular Sciences (M. T. Hyvönen), the Federation of Finnish Insurance Companies (P. T. Kovanen and M. Ala-Korpela), the Finnish Cultural Foundation (M. T. Hyvönen and K. Öörni), the Juselius Foundation (P. T. Kovanen and M. Ala-Korpela), the Research Foundation of Orion Corporation (M. T. Hyvönen), and the University of Oulu (M. T. Hyvönen).

REFERENCES

Abrams, F. S., A. Chattopadhyay, and E. London. 1992. Determination of the location of fluorescent probes attached to fatty acids using parallax analysis of fluorescence quenching: effect of carbonyl ionization state and environment on depth. *Biochemistry.* 31:5322–5327.

Akutsu, H., and T. Nagamori. 1991. Conformational analysis of the polar headgroup in phosphatidylcholine bilayers. A structural change induced by cations. *Biochemistry.* 30:4510–4516.

Alper, H. E., D. Bassolino-Klimas, and T. R. Stouch. 1993. The limiting behavior of water hydrating a phospholipid monolayer: a computer simulation study. *J. Chem. Phys.* 99:5547–5559.

Apitz-Castro, R., M. K. Jain, and G. H. De Haas. 1982. Origin of the latency phase during the action of phospholipase A_2 on unmodified phosphatidylcholine vesicles. *Biochim. Biophys. Acta.* 688:349–356.

Basáñez, G., J.-L. Nieva, F. M. Goñi, and A. Alonso. 1996. Origin of the lag period in the phospholipase C cleavage of phospholipids in membranes. Concomitant vesicle aggregation and enzyme activation. *Biochemistry.* 35:15183–15187.

Bassolino-Klimas, D., H. E. Alper, and T. R. Stouch. 1995. Mechanism of solute diffusion through lipid bilayer membranes by molecular dynamics simulation. *J. Am. Chem. Soc.* 117:4118–4129.

Bell, J. D., and R. L. Biltonen. 1992. Molecular details of the activation of soluble phospholipase A_2 on lipid bilayers. *J. Biol. Chem.* 267: 11046–11056.

Bell, J. D., M. Burnside, J. A. Owen, M. I. Royall, and M. L. Baker. 1996. Relationships between bilayer structure and phospholipase A_2 activity: interactions among temperature, diacylglycerol, lysolecithin, palmitic acid, and dipalmitoylphosphatidylcholine. *Biochemistry.* 35:4945–4955.

Belohorcová, K., J. H. Davis, T. B. Woolf, and B. Roux. 1997. Structure and dynamics of an amphiphilic peptide in a lipid bilayer: a molecular dynamics study. *Biophys. J.* 73:3039–3055.

Bent, E. D., and J. D. Bell. 1995. Quantification of the interactions among fatty acid, lysophosphatidylcholine, calcium, dimyristoylphosphatidylcholine vesicles, and phospholipase A_2. *Biochim. Biophys. Acta.* 1254: 349–360.

Berendsen, H. J. C., B. Egberts, S. J. Marrink, and P. Ahlström. 1992. Molecular dynamics simulations of phospholipid membranes and their interaction with phospholipase A_2, *In* Membrane Proteins: Structures, Interactions and Models. Pullman, A., Jortner, J., and Pullman, B., editors. Kluwer Academic Publishers, Dordrecht, The Netherlands. 457–470.

Berger, O., O. Edholm, and F. Jähnig. 1997. Molecular dynamics simulations of a fluid bilayer of dipalmitoylphosphatidylcholine at full hydration, constant pressure and constant volume. *Biophys. J.* 72:2002–2013.

Brooks, B. R., R. E. Bruccoleri, B. D. Olafson, D. J. States, S. Swaminathan, and M. Karplus. 1983. CHARMM: a program for macromolecular energy, minimization, and dynamics calculations. *J. Comput. Chem.* 4:187–217.

Burack, W. R., and R. L. Biltonen. 1994. Lipid bilayer heterogeneities and modulation of phospholipase A_2 activity. *Chem. Phys. Lipids.* 73: 209–222.

Burack, W. R., A. R. G. Dibble, M. M. Allietta, and R. L. Biltonen. 1997. Changes in vesicle morphology induced by lateral phase separation modulate phospholipase A_2 activity. *Biochemistry.* 36:10551–10557.

Burack, W. R., M. E. Gadd, and R. L. Biltonen. 1995. Modulation of phospholipase A_2: identification of an inactive membrane-bound state. *Biochemistry.* 34:14819–14828.

Burack, W. R., Q. Yuan, and R. L. Biltonen. 1993. Role of lateral phase separation in the modulation of phospholipase A_2 activity. *Biochemistry.* 32:583–589.

Chiu, S.-W., M. Clark, V. Balaiji, S. Subramaniam, H. L. Scott, and E. Jakobsson. 1995. Incorporation of surface tension into molecular dynamics simulation of an interface: a fluid phase lipid bilayer membrane. *Biophys. J.* 69:1230–1245.

Damodaran, K. V., and K. M. Merz, Jr. 1994. A comparison of DMPC- and DLPE-based lipid bilayers. *Biophys. J.* 66:1076–1087.

Essmann, U., and M. L. Berkowitz. 1999. Dynamical properties of phospholipid bilayers from computer simulation. *Biophys. J.* 76:2081–2089.

Essmann, U., L. Perera, and M. L. Berkowitz. 1995. The origin of the hydration interaction of lipid bilayers from MD simulation of dipalmitoylphosphatidylcholine membranes in gel and liquid crystalline phases. *Langmuir.* 11:4519–4531.

Feller, S. E., and R. W. Pastor. 1996. On simulating lipid bilayers with an applied surface tension: periodic boundary conditions and undulations. *Biophys. J.* 71:1350–1355.

Feller, S. E., and R. W. Pastor. 1999. Constant surface tension simulations of lipid bilayers: the sensitivity of surface areas and compressibilities. *J. Chem. Phys.* 111:1281–1287.

Feller, S. E., R. W. Pastor, A. Rojnuckarin, S. Bogusz, and B. R. Brooks. 1996. Effect of electrostatic force truncation on interfacial and transport properties of water. *J. Phys. Chem.* 100:17011–17020.

Flewelling, R. F., and W. L. Hubbel. 1986. The membrane dipole potential in a total membrane potential model. *Biophys. J.* 49:541–552.

Gawrisch, K., D. Ruston, J. Zimmerberg, V. A. Parsegian, R. P. Rand, and N. Fuller. 1992. Membrane dipole potentials, hydration forces, and the ordering of water at membrane surfaces. *Biophys. J.* 61:1213–1223.

Gelb, M. H., W. Cho, and D. C. Wilton. 1999. Interfacial binding of secreted phospholipases A_2: more than electrostatics and a major role of tryptophan. *Curr. Opin. Struct. Biol.* 9:428–432.

Ghomashchi, F., B.-Z. Yu, O. Berg, M. K. Jain, and M. H. Gelb. 1991. Interfacial catalysis by phospholipase A_2: substrate specificity in vesicles. *Biochemistry.* 30:7318–7329.

Grandbois, M., H. Clausen-Schaumann, and H. Gaub. 1998. Atomic force microscope imaging of phospholipid bilayer degradation by phospholipase A_2. *Biophys. J.* 74:2398–2404.

Hamilton, J. A. 1995. ^{13}C NMR studies of the interactions of fatty acids with phospholipid bilayers, plasma lipoproteins, and proteins. *In* Carbon-13 NMR Spectroscopy of Biological Systems. Nicolau Beckmann, editor. Academic Press Inc., London. 117–159.

Han, S. K., E. T. Yoon, D. L. Scott, P. B. Sigler, and W. Cho. 1997. Structural aspects of interfacial adsorption. A crystallographic and site-directed mutagenesis study of the phospholipase A_2 from the venom of *Agkistrodon piscivorus piscivorus. J. Biol. Chem.* 272:3573–3582.

Henshaw, J. B., C. A. Olsen, A. R. Farnbach, K. H. Nielson, and J. D. Bell. 1998. Definition of specific roles of lysolecithin and palmitic acid in altering the susceptibility of dipalmitoylphosphatidylcholine bilayers to phospholipase A_2. *Biochemistry.* 37:10709–10721.

Hønger, T., K. Jørgensen, R. L. Biltonen, and O. G. Mouritsen. 1996. Systematic relationship between phospholipase A_2 activity and dynamic lipid bilayer microheterogeneity. *Biochemistry.* 35:9003–9006.

Hyvönen, M., T. T. Rantala, and M. Ala-Korpela. 1997. Structure and dynamic properties of diunsaturated 1-palmitoyl-2-linoleoyl-*sn*-glycero-3-phosphatidylcholine lipid bilayer from molecular dynamics simulation. *Biophys. J.* 73:2907–2923.

Jähnig, F. 1996. What is the surface tension of a lipid bilayer membrane? *Biophys. J.* 71:1348–1349.

Jain, M. K., and G. H. de Haas. 1983. Activation of phospholipase A_2 by freshly added lysophospholipids. *Biochim. Biophys. Acta.* 736:157–162.

Jain, M. K., and D. V. Jahagirdar. 1985. Action of phospholipase A_2 on bilayers. Effect of fatty acid and lysophospholipid additives on the kinetic parameters. *Biochim. Biophys. Acta.* 814:313–318.

Jones, S. T., P. Ahlström, H. J. C. Berendsen, and R. W. Pickersgill. 1993. Molecular dynamics simulation of a phospholipase A_2-substrate complex. *Biochim. Biophys. Acta.* 1162:135–142.

Jorgensen, W. L., J. Chandrasekhar, J. D. Madura, R. W. Impey, and M. L. Klein. 1983. Comparison of simple potential functions for simulating liquid water. *J. Chem. Phys.* 79:926–935.

Laaksonen, L. 1992. A graphics program for the analysis and display of molecular dynamics trajectories. *J. Mol. Graphics.* 10:33–34.

Lehtonen, J. Y. A., and P. K. J. Kinnunen. 1995. Phospholipase A_2 as a mechanosensor. *Biophys. J.* 68:1888–1894.

Lopez Cascales, J. J., H. J. C. Berendsen, and J. Garcia de la Torre. 1996b. Molecular dynamics simulation of water between two charged layers of dipalmitoylphosphatidylserine. *J. Phys. Chem.* 100:8621–8627.

Lopez Cascales, J. J., J. Garcia de la Torre, S. J. Marrink, and H. J. C. Berendsen. 1996a. Molecular dynamics simulation of a charged biological membrane. *J. Chem. Phys.* 104:2713–2720.

Marrink, S. J., M. Berkowitz, and H. J. C. Berendsen. 1993. Molecular dynamics simulation of a membrane/water interface: the ordering of water and its relation to the hydration force. *Langmuir.* 9:3122–3131.

Marrink, S. J., F. Jähnig, and H. J. C. Berendsen. 1996. Proton transport across transient single-file water pores in a lipid membrane studied by molecular dynamics simulations. *Biophys. J.* 71:632–647.

McLean, L. R., K. A. Hagaman, and W. S. Davidson. 1993. Role of lipid structure in the activation of phospholipase A_2 by peroxidized phospholipids. *Lipids.* 28:505–509.

Murakami, M., Y. Nakatani, G. Atsumi, K. Inoue, and I. Kudo. 1997. Regulatory functions of phospholipase A_2. *Critical Reviews in Immunology.* 17:225–283.

Roux, B. 1996. Commentary: surface tension of biomembranes. *Biophys. J.* 71:1346–1347.

Schlenkrich, M., J. Brickmann, A. D. MacKerell, Jr., and M. Karplus. 1996. An empirical potential energy function for phospholipids: criteria for parameter optimization and applications. *In* Biological Membranes: A Molecular Perspective from Computation and Experiment. K. M. Merz and B. Roux, editors. Birkhäuser, Boston. 31–82.

Scott, D. L., and P. B. Sigler. 1994. Structure and catalytic mechanism of secretory phospholipases A_2. *Adv. Protein Chem.* 45:53–88.

Seelig, J., and W. Niederberger. 1974. Deuterium-labeled lipids as structural probes in liquid crystalline bilayers. A deuterium magnetic resonance study. *J. Am. Chem. Soc.* 96:2069–2072.

Sheffield, M. J., B. L. Baker, N. L. Owen, M. L. Baker, and J. D. Bell. 1995. Enhancement of *Agkistrodon piscivorus piscivorus* venom phospholipase A_2 activity toward phosphatidylcholine vesicles by lysolecithin and palmitic acid: studies with fluorescent probes of membrane structure. *Biochemistry.* 34:7796–7806.

Shinoda, W., M. Shimizu, and S. Okazaki. 1998. Molecular dynamics study on electrostatic properties of a lipid bilayer: polarization, electrostatic potential, and the effects on structure and dynamics of water near the interface. *J. Phys. Chem.* 102:6647–6654.

Simon, S. A., and T. J. McIntosh. 1989. Magnitude of the solvation pressure depends on dipole potential. *Proc. Natl. Acad. Sci. U.S.A.* 86:9263–9267.

Tieleman, D. P., and H. J. C. Berendsen. 1996. Molecular dynamics simulations of a fully hydrated dipalmitoylphosphatidylcholine bilayer with different macroscopic boundary conditions and parameters. *J. Chem. Phys.* 105:4871–4880.

Tieleman, D. P., and H. J. C. Berendsen. 1998. A molecular dynamics study of the pores formed by *Escherichia coli* OmpF porin in a fully hydrated palmitoyloleoylphosphatidylcholine bilayer. *Biophys. J.* 74: 2786–2801.

Tieleman, D. P., S. J. Marrink, and H. J. C. Berendsen. 1997. A computer perspective of membranes: molecular dynamics studies of lipid bilayer systems. *Biochim. Biophys. Acta.* 1331:235–270.

Tobias, D. J., K. Tu, and M. L. Klein. 1997. Atomic-scale molecular dynamics simulations of lipid membranes. *Curr. Opin. Colloid Interface Sci.* 2:15–26.

van Gunsteren, W. F., and H. J. C. Berendsen. 1977. Algorithms for macromolecular dynamics and constraint dynamics. *Mol. Phys.* 34: 1311–1327.

Venable, R. M., B. R. Brooks, and R. W. Pastor. 2000. Molecular dynamics simulations of gel ($L_{\beta I}$) phase lipid bilayers in constant pressure and constant surface area ensembles. *J. Chem. Phys.* 112:4822–4832.

Voglino, L., T. J. McIntosh, and S. A. Simon. 1998. Modulation of the binding of signal peptides to lipid bilayers by dipoles near the hydrocarbon-water interface. *Biochemistry.* 37:12241–12252.

Volwerk, J. J., P. C. Jost, G. H. de Haas, and O. H. Griffith. 1986. Activation of porcine pancreatic phospholipase A_2 by the presence of negative charges at the lipid-water interface. *Biochemistry.* 25: 1726–1733.

Waite, M. 1996. Phospholipases. *In* Biochemistry of Lipids, Lipoproteins and Membranes. D. E. Vance and J. Vance, editors. Elsevier, Amsterdam. 211–236.

Watanabe, K., M. Ferrario, and M. L. Klein. 1988. Molecular dynamics study of a sodium octanoate micelle in aqueous solution. *J. Phys. Chem.* 92:819–821.

Wilson, M. A., and A. Pohorille. 1996. Mechanism of unassisted ion transport across membrane bilayers. *J. Am. Chem. Soc.* 118:6580–6587.

Wymore, T., and T. C. Wong. 1999. Molecular dynamics study of substance P peptides partitioned in a sodium dodecylsulfate micelle. *Biophys. J.* 76:1213–1227.

Zhou, F., and K. Schulten. 1996. Molecular dynamics study of phospholipase A_2 on a membrane surface. *Proteins: Struct., Funct., Genet.* 25:12–27.

Zubrzycki, I. Z., Y. Xu, M. Madrid, and P. Tang. 2000. Molecular dynamics simulations of a fully hydrated dimyristoylphosphatidylcholine membrane in liquid-crystalline phase. *J. Chem. Phys.* 112:3437–3441.